

# Atomic oxygen impacts on Materials International Space Station Experiment (MISSE)-16 flight samples

Samuel A. Westrick<sup>(1)</sup>, Elena A. Plis<sup>(2)</sup>, Jainisha R. Shah<sup>(3)</sup>, Sydney Collman<sup>(4)</sup>, Ryan C. Hoffman<sup>(3)</sup>, and Heather Cowardin<sup>(5)</sup>

<sup>(1)</sup> Universities Space Research Association at Air Force Research Laboratories, Kirtland AFB, Albuquerque, NM 87117, USA, AFRL.RVborgmailbox@us.af.mil

<sup>(2)</sup> Georgia Tech Research Institute (GTRI), 925 Dalney St NW, Atlanta, Georgia 30318, USA, Elena.Plis@gtri.gatech.edu

<sup>(3)</sup> Air Force Research Laboratories, Kirtland AFB, Albuquerque, NM 87117, USA, RVBorgmailbox@us.af.mil

<sup>(4)</sup> Assurance Technology Corporation, 84 South St, Carlisle, MA 01741, USA, collman@assurtech.com

<sup>(5)</sup> NASA Orbital Debris Program Office, 2101 E NASA Pkwy, Houston, TX 77058, USA, heather.cowardin@nasa.gov

## Abstract

A variety of materials consisting of polyimides, polyethylene terephthalates (PETs), fiber reinforced polymers, and polyhedral oligomeric silsesquioxanes (POSS) were on the exterior of the International Space Station (ISS) as part of Materials International Space Station Experiment (MISSE)-16. Samples on the side of the ISS pointing in the direction of the spacecraft's motion (the ram direction) were observed for effects due to atomic oxygen (AO). The erosion yield of select materials from MISSE-16 is reported, as well as their variation in surface roughness due to AO erosion.

Trade names and trademarks are used in this paper for identification only. Their usage does not constitute an official endorsement, either expressed or implied, by the National Aeronautics and Space Administration.

## 1 Introduction

The exterior of spacecraft can be damaged by constituents of the space environment as physical, chemical, and optical properties of materials can alter over time. How the properties of materials evolve while in orbit is crucial to understand for the longevity of a spacecraft mission. The Materials International Space Station Experiment Flight Facility (MISSE-FF) has exposed many materials to the low Earth orbit (LEO) environment to observe their durability and performance.

Atomic oxygen (AO) exists in LEO and is the most abundant species from 160km to 650km [1,2]. It is known to erode materials, especially polymers. LEO atomic oxygen has enough energy ( $4.5\pm 1\text{eV}$ ) to react with most organic materials and break bonds of most organic polymers with sufficient flux to cause oxidative erosion. Erosion could lead to degradation of the polymers which could contribute to the small particle orbital debris population.

MISSE-16 launched in August 2022 and was delivered to the International Space Station (ISS), where it was then exposed to the space environment for six months. It was the first MISSE to incorporate a

camera to record in-situ images of material samples as they were exposed to the space environment. The materials onboard consisted of different classes of polymers. Several polyimides of the Kapton® family (Kapton® HN, Kapton® CR, Kapton® CS, Kapton® WS, Kapton® TF, Kapton® XC), as well as mylars (Mylar® M021 and Melinex® 454) were in the MISSE-FF. Other polymers onboard included carbon fiber reinforced polymer (CFRP), glass fiber reinforced polymer (GFRP), Zenite®, Thermalbright®N, DR9, and Corin® XLS.

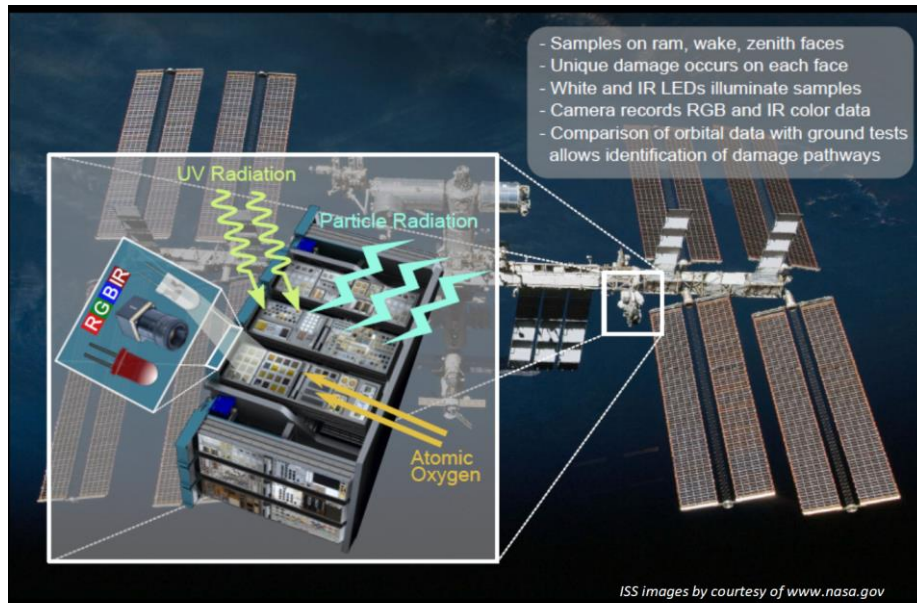


Fig. 1. Materials International Space Station Experiment (MISSE) Flight Facility (MISSE-FF)

Polyimides (Kapton® films particularly) are ubiquitous in spacecraft construction for uses such as multi-layered insulation (MLI) blankets [3-6] as they are durable, flexible, chemically inert, and can withstand extreme temperature and radiation conditions [7]. Mylar, a polyethylene terephthalate (PET), is utilized for MLI blankets on the exterior of spacecraft for passive thermal control purposes [8-10]. Polyhedral oligomeric silsesquioxane (POSS) has been proposed as enhancement materials within polyimide (PI)-based nanocomposites to improve their thermo-mechanical and AO-resistant properties [11,12]. Upon AO exposure, POSS-PI forms a surface layer of silicon dioxide (SiO<sub>2</sub>) that is resistant to AO-erosion, reducing AO erosion of the bulk (i.e., PI) matrix. Thermalbright®N is one such material that incorporates POSS.

1"x1" Samples were located on the ram side, the zenith side, and the wake side of the spacecraft where they were exposed to atomic oxygen, ultraviolet (UV) radiation, and electron bombardment. The samples were transported back to Earth in April 2023, and post-flight analysis of the samples was performed.

## 2 Methodology

### 2.1 Erosion Yield

ASTM E2089 is the standard for atomic oxygen tests characterizing changes in material mass and thickness for ground laboratories [13]. While samples were exposed to atomic oxygen in space, the standard was followed as closely as possible to derive the erosion yield and produce comparable results.

The decision to study erosion yield was not made until after the samples were already in orbit, and as such there was no recorded mass data for the samples before they were placed in orbit. As such, flight duplicate samples were created to record pristine mass. Once the samples located on the ram side were received, the pristine flight-duplicate samples and the flight samples were placed in a APTline™ VD vacuum drying oven. All the samples were stored at <200 mTorr at room temperature for 48 hours so water vapor mass could outgas and not contribute to mass measurements. The mass of the samples were then recorded with a Cole-Parmer PA – 1241 analytical balance (readability 0.0001g, repeatability 0.0002g) quickly after removal from the drying oven to mitigate water vapor absorption.

While the pristine samples were cut to the same dimensions as the MISSE samples exposed to AO, minor differences in size will create differences in mass that can be greater than the difference in mass due to AO erosion. As such, ImageJ, an image processing software, was utilized to evaluate difference in the materials optically via pixel examination. By counting the number of pixels that constructs a sample and using a known distance in the image, the area of the samples may be precisely calculated. Knowing the density of a material, the recorded mass of the pristine sample can then be corrected accounting for any difference in sample area.



Fig 2. ImageJ analysis of pristine Kapton® XC sample used to estimate area for erosion yield calculations  
The erosion rate  $E_y$  (presented as  $\text{cm}^3/\text{atom}$ ) can be calculated with Eq. 1:

$$E_y = \Delta M_s / (A_s * \rho_s * F_k) \quad \text{Eq. 1}$$

Where  $\Delta M_s$  is the difference in mass between the pristine sample and spaceflight sample (g),  $A_s$  is the area of the spaceflight sample that was exposed to AO ( $4.551 \text{ cm}^2$ ),  $\rho_s$  is the density of the sample ( $\text{g}/\text{cm}^3$ ), and  $F_k$  is the fluence of atom oxygen the spaceflight samples received ( $\text{atoms}/\text{cm}^2$ ). The fluence ( $3.07\text{E}+20 \text{ atoms}/\text{cm}^2$ ) was recorded using a witness Kapton® H sample that was on the ram side of MISSE-FF with samples.

## 2.2 Surface Roughness

The surface roughness of the returned MISSE-16 samples was measured using a Keyence VHX-7000 microscope operating in 3D mode. Each sample displayed edges that were not exposed to atomic oxygen as they were shielded by MISSE's aluminum frame carriers ( $\sim 1.9\text{cm}^2$  of sample surface area was shielded). As such, the frame-covered area for each sample was measured as the surface roughness of the pristine material. Four measurements were taken at the edges and for the area of the samples exposed to atomic oxygen, five measurements were taken in different locations. The locations of the measurements are shown in Fig. 3

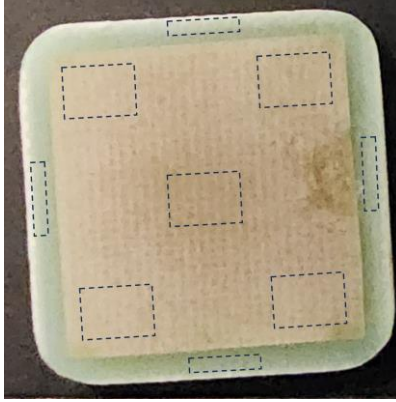


Fig 3. Representative schematic of surface roughness evaluation. The material featured here is GFRP.

Analysis of surface roughness utilized two different filters, the S-filter and the L-filter. The S-filter was used to remove small-scale roughness components (known as a low-pass filter), while the L-filter was used to eliminate large-scale wave components (high-pass filter). Both the S-filter and L-filter were set to 50  $\mu\text{m}$  and were used together to form a band-pass filter.

### 3 Results and Discussion

A material's erosion yield is indicative of its durability in a LEO orbit and gives spacecraft designers insight into which materials to use or how much of a material to use to ensure the material performs its function successfully throughout the entirety of the mission. Erosion yield can also assist in determining a material's susceptibility to creating debris via erosion. Table 1 below contains the erosion yield values for MISSE-16 materials calculated as discussed in section 2.1. The error bars are calculated taking into account the readability of the scale and the uncertainty in the calculation of the area.

Table 1. Erosion yield of select MISSE-16 polymers

Material	$E_y$ ( $\text{cm}^3/\text{atom}$ )	Material	$E_y$ ( $\text{cm}^3/\text{atom}$ )
Kapton <sup>®</sup> XC	$3.07 \pm 0.51\text{E-}24$	Zenite <sup>®</sup>	$8.89 \pm 2.3\text{E-}25$
DR9	$9.46 \pm 0.57\text{E-}24$	Melinex <sup>®</sup> 454	$1.25 \pm 0.04\text{E-}23$
CFRP	$5.59 \pm 0.34\text{E-}24$	Mylar <sup>®</sup> M021	$1.32 \pm 0.05\text{E-}23$
GFRP	$4.81 \pm 0.91\text{E-}24$	Thermalbright <sup>®</sup> N	$2.77 \pm 5.96\text{E-}25$

From Table 1 it is deduced that the PETs (Mylar<sup>®</sup> M021 and Melinex<sup>®</sup> 454) are more prone to AO-induced erosion than other polymers. The POSS characteristic of forming a silicon-dioxide protective layer appears to be effective as Thermalbright<sup>®</sup>N exhibited an erosion yield an order of magnitude less than the majority of the samples studied. The associated error is greater than 100%. This is only to say that the erosion yield of the Thermalbright<sup>®</sup>N sample is too small to be accurately determined given the uncertainties in area and mass, and not that Thermalbright<sup>®</sup>N potentially gained mass. The lower erosion yield in Zenite<sup>®</sup> may be attributed to the glass reinforcement present in the polymer. The polyimides (Kapton<sup>®</sup> XC and DR9) as well as CFRP and GFRP had erosion yields on the same order of magnitude as Kapton<sup>®</sup> H ( $3.0 \times 10^{-24} \text{cm}^3/\text{atom}$ ). However, with the exception of Kapton<sup>®</sup> XC, it is clear that they experienced more erosion than the standard Kapton<sup>®</sup> H.

The change in surface roughness of select MISSE-16 materials as a result of AO-induced erosion are reported in Table 2 below. The surface roughness is reported as the root mean square (rms) of the surface.

Table 2. Change in surface roughness of select MISSE-16 polymers

Material	Pristine ( $\mu\text{m}$ )	AO-exposed ( $\mu\text{m}$ )	Material	Pristine ( $\mu\text{m}$ )	AO-exposed ( $\mu\text{m}$ )
Kapton <sup>®</sup> XC	2.60	3.14	Zenite <sup>®</sup>	1.75	1.98
DR9	1.36	2.96	Melinex <sup>®</sup> 454	3.70	0.81
CFRP	3.54	7.95	Mylar <sup>®</sup> M021	0.52	0.54
GFRP	0.74	1.73	Thermalbright <sup>®</sup> N	0.75	1.93

The increase in surface roughness observed in most of the selected materials is expected. As a spacecraft collides with atomic oxygen in orbit, the atomic oxygen, relative to the ram surface, is mainly coming from one direction. This will cause pits and cones to form on the material surface as the location of atomic oxygen impact and therefore erosion is random. As erosion of one location is independent of any other location and because atomic oxygen arrives at random locations on the surface, the surface roughness of a material will follow Poisson statistics and increase relative to the square root of the fluence [1,14]. The decrease in surface roughness observed in Melinex<sup>®</sup> 454 is intriguing. Other constituents of the space environment may contribute to the increased smoothness. Many studies [15-17] have found that electron irradiation of PETs has resulted in the decrease of surface roughness. An increased level of crosslinking in electron-irradiated polymers may contribute to a smoothing of the surface, but further investigation is needed to determine the mechanisms that alter surface texture.

#### 4 Conclusion

MISSE-16 conducted a comprehensive investigation into the effects of atomic oxygen exposure on a variety of polymer materials, including polyimides, PETs, fiber-reinforced polymers, and POSS. The erosion caused by atomic oxygen can lead to material degradation and possibly contribute to the small particle orbital debris population, which poses challenges for spacecraft durability and safety. Erosion yield values were determined for various materials, providing insights into their durability in LEO and their potential for generating debris through erosion. Notably, PETs, such as Mylar<sup>®</sup> M021 and Melinex<sup>®</sup> 454, exhibited higher erosion yields, indicating their susceptibility to AO-induced erosion. Thermalbright<sup>®</sup> N (a POSS material) appears to be effective in mitigating AO erosion. This finding suggests the potential of incorporating POSS into polyimides to enhance AO-resistant properties of materials in spacecraft construction.

Most materials examined in this paper exhibited an increase in surface roughness due to the random impact of atomic oxygen. Increased surface roughness due to AO-erosion can create an increase in diffuse reflectance as the texturing of the surface scatters light [1]. If these polymers existed as debris in LEO, the change in optical properties due to the increase in surface roughness would be useful knowledge for the debris-tracking community. Melinex<sup>®</sup> 454 displayed a decrease in surface roughness, which warrants further investigation.

Research of spacecraft material property changes is essential for ensuring the longevity and safety of spacecraft missions in the challenging LEO environment, where atomic oxygen remains a significant concern. Further research and analysis will be necessary to fully understand the observed surface roughness changes and their implications for spacecraft materials.

## 5 Acknowledgements

This work was partially supported by the Air Force Office of Scientific Research Physics of Remote Sensing Program under the direction of Dr. Michael Yakes (LRIR # 20RVCOVR024). The authors would like to acknowledge the support of Air Force Research Laboratory (AFRL) Scholars Professional 2023 program at Kirtland Air Force Base, administered by the Universities Space Research Association through a cooperative agreement with AFRL. The authors also would like to thank Mr. Timothy R. Scott from DuPont de Nemours, Inc., for providing PI materials for this research.

## 6 Disclaimers

The views expressed are those of the authors and do not necessarily reflect the official policy or position of the U.S. Department of the U.S. Air Force, the U.S. Department of Defense, or the U.S. Government. The appearance of external hyperlinks does not constitute endorsement by the U.S. Department of Defense (DOD) of the linked websites or the information, products, or services contained therein. The DOD does not exercise any editorial, security, or other control over the information you may find at these locations. The authors acknowledge that their work does not infringe on any copyright and grant USRA permission to include this work in any and all materials associated with this conference.

## 7 References

1. NASA, NASA-HDBK6024, *Spacecraft Polymers Atomic Oxygen Durability Handbook*. 2014.
2. Pisacane, Vincent L. *The space environment and its effects on space systems*. American Institute of aeronautics and Astronautics, 2008.
3. Akram, S., Castellon, J., Kai, Z., Agnel, S., Haba, J.-P., Nazir, M.T.: Dielectric properties and modeling of multilayer polyimide nanocomposite to highlight the impact of nanoparticles dispersion. *IEEE Transactions on Dielectrics and Electrical Insulation* 27(4), 1238-1246 (2020)
4. Gouzman, I., Grossman, E., Verker, R., Atar, N., Bolker, A., Eliaz, N.: Advances in polyimide-based materials for space applications. *Advanced materials* 31(18), 1807738 (2019)
5. Bovesecchi, G., Corasaniti, S., Costanza, G., Piferi, F.P., Tata, M.E.: Deployment of solar sails by joule effect: Thermal analysis and experimental results. *Aerospace* 7(12), 180 (2020)
6. Spencer, D.A., Johnson, L., Long, A.C.: Solar sailing technology challenges. *Aerospace Science and Technology* 93, 105276 (2019)
7. Dupont™: Dupont™ Kapton® Summary of Properties (2017)
8. Kang, C.-S.: Multilayer insulation for spacecraft applications. In: *COSPAR Colloquia Series*, vol. 10, pp. 175–179 (1999). Elsevier
9. Khalil, E.E., Farag, A.M., ElZahaby, A.M., Khali, M.K., Wafi, T.Z.: Parametric study of multi-layer insulation optical properties effect on spacecraft thermal control system during flight missions. In: *2018 Joint Propulsion Conference*, p. 4615 (2018)
10. Pryor, W., Vagvolgyi, B.P., Gallagher, W.J., Deguet, A., Leonard, S., Whitcomb, L.L., Kazanzides, P.: Experimental evaluation of teleoperation interfaces for cutting of satellite insulation. In: *2019 International Conference on Robotics and Automation (ICRA)*, pp. 4775–4781 (2019). IEEE

11. Lei, X.-F., Qiao, M.-T., Tian, L.-D., Yao, P., Ma, Y., Zhang, H.-P., Zhang, Q.-Y.: Improved space survivability of polyhedral oligomeric silsesquioxane (poss) polyimides fabricated via novel poss-diamine. *Corrosion Science* 90, 223–238 (2015)
12. Vij, V., Haddad, T.S., Yandek, G.R., Ramirez, S.M., Mabry, J.M.: Synthesis of aromatic polyhedral oligomeric silsesquioxane (poss) dianilines for use in high-temperature polyimides. *Silicon* 4, 267–280 (2012)
13. ASTM E2089-15: Standard Practices for Ground Laboratory Atomic Oxygen Interaction Evaluation of Materials for Space Applications. Standard, ASTM International, West Conshohocken, PA, Mar. 2015 (2020).
14. Banks, B.; Miller, S; de Groh, K.; Chan, A.; Sahota, M. (November 26-30, 2001). *The Development of Surface Roughness and Implications for Cellular Attachment in Biomedical Applications*. Paper presented at the Materials Research Society 2001 Fall Meeting. Boston, MA. Also published as NASA/TM—2001-211288.
15. Plis, E., Bengtson, M., Engelhart, D. P., Badura, G., Scott, T., Cowardin, H., ... & Horne, S. (2022). Characterization of novel spacecraft materials under high energy electron and atomic oxygen exposure. In *AIAA SciTech 2022 Forum* (p. 0797).
16. Chinaglia, D., Constantino, C., Aroca, R., and Oliveira Jr, O., "Surface modifications on Teflon FEP and Mylar C induced by alow energy electron beam: A Raman and FTIR spectroscopic study," *Molecular Crystals and Liquid Crystals*, Vol. 374, No. 1, 2002, pp. 577–582.
17. Lee, E., Lewis, M., Blau, P., and Mansur, L., "Improved surface properties of polymer materials by multiple ion beam treatment," *Journal of Materials Research*, Vol. 6, No. 3, 1991, pp. 610–628.